

## E-1-4

## Evaluation of base-collector capacitance in submicron buried metal heterojunction bipolar transistors

Yasuyuki Miyamoto, Toshiki Arai, Shigeharu Yamagami, Koji Matsuda, and Kazuhito Furuya

Department of Physical Electronics, Tokyo Institute of Technology  
2-12-1 O-okayama, Meguro-ku, Tokyo 152-8552, Japan  
Phone: +81-3-5734-2572, Fax: +81-3-5734-2907, E-mail: [miya@pe.titech.ac.jp](mailto:miya@pe.titech.ac.jp)

### 1. Introduction

Reduction of base-collector capacitance ( $C_{BC}$ ) is essential for high-speed operation of heterojunction bipolar transistors. Usually reduction of  $C_{BC}$  is evaluated by increase of maximum oscillation frequency ( $f_{MAX}$ ). Thus, decrease of intrinsic  $C_{BC}$  ( $C_{BCin}$ ) becomes most important [1]. However, future scaling of HBT [2] requires reduction of total  $C_{BC}$  ( $C_{BCT}$ ) for increase of cutoff frequency ( $f_T$ ). Moreover, smaller  $C_{BCT}$  provides smaller feedback capacitance, results in larger maximum available gain [1].

In this report, we describe base-collector capacitance in submicron buried metal heterojunction bipolar transistors (BMHBT)[3], which is our proposed structure for reduction of  $C_{BCT}$ . When emitter width is 0.3  $\mu\text{m}$ ,  $C_{BCT}$  was less than 1 fF. To our knowledge, this is smallest  $C_{BCT}$  in HBT.

### 2. Device and microwave performance

In a structure of BMHBT, metal wires buried in semiconductor extract electrons as shown in Fig. 1. Because buried metal wires replace conventional sub-collector layer and no conducting region exists under the extrinsic base region, extrinsic  $C_{BC}$  ( $C_{BCext}$ ) can be eliminated, results in small  $C_{BCT}$ . We reported the fabrication process of submicron BMHBT previously [4].

Common emitter characteristics and microwave characteristics of BMHBT with emitter area of  $0.3 \times 1.5 \mu\text{m}^2$  are shown in Fig. 2 and 3. The pad capacitances were extracted. As shown in Fig. 3, estimated  $f_T$  and  $f_{MAX}$  are 82 GHz and 200 GHz, respectively.

$C_{BCT}$  was estimated by imaginary part of  $Y_{12}$  parameter in a low frequency region as shown in open circles of Fig. 4. Estimated  $C_{BCT}$  decreased with reduction of emitter area. When emitter width was 0.3  $\mu\text{m}$ , observed  $C_{BCT}$  was 0.95 fF.

### 3. Analysis by elements

In case of BMHBT, observed  $C_{BCT}$  should be equal to  $C_{BCin}$ . To confirm this expectation, Elements of equivalent circuit (Fig. 5) were estimated in the device with emitter area of  $0.5 \times 2.5 \mu\text{m}^2$ . Collector resistance  $R_{CC}$  and sum of emitter resistance were estimated from Z parameters [5]. Dynamic emitter resistance  $r_E$  and contact resistance  $R_{EE}$  were divided from sum of emitter resistance by collector current dependence of emitter resistance. Emitter charging time was estimated by collector current dependence of  $f_T$ . Base emitter capacitance  $C_{BE}$  was estimated from emitter charging time and  $r_E$ . Base resistance including contact resistance was

estimated by sheet resistance and contact resistivity measured by the transmission line method. As base-collector capacitance, we assume  $C_{BCT}$  is equal to  $C_{BCin}$ . Estimated elements under  $I_c = 3.5 \text{ mA}$  and  $V_{CE} = 5 \text{ V}$  are shown in Table 1. Figure 6 shows simulated gains with measured data. From Fig. 6, we could explain observed result without  $C_{BCext}$ .

### 4. Discussion

From Table 1, major reason of present poor  $f_T$  can be explained by high  $R_{CC}$ . We estimated that the high  $R_{CC}$  was due to poor contact between tungsten and metal for wiring because oxide on the tungsten surface was formed by ashing process. Toward next trials, we confirmed that oxide could be removed by BHF treatment. Estimated  $r_E$  is 10 times higher than emitter resistance calculated from collector current. This might be explained by space charge in the emitter because we used high current density ( $250 \text{ kA/cm}^2$ ). Observed  $C_{BCT}$  was larger than estimation from emitter area as shown in the line of theory in Fig. 4. Because  $C_{BCT}$  consisted from  $C_{BCin}$  only, this could be explained by conductive region around metal wires. When we assume that conductive region has same width around metal wires, observed  $C_{BCT}$  can be explained by width of conductive region of 0.25  $\mu\text{m}$  as shown in Fig. 4. The temperature of buried growth was 585  $^\circ\text{C}$  at present trial. When we used 600  $^\circ\text{C}$  as growth temperature [6], observed width of conductive region was estimated as 1  $\mu\text{m}$ . In separate experiment using C-V measurement, we confirmed that present process did not make additional carrier around grown interface. Moreover, present resistivity of the tungsten was 10 times higher than that of bulk. Thus diffusion of impurity from tungsten wires is one of the possible reasons of the conductive region. Improvement of purity of tungsten might reduce the width of the conductive region.

### 5. Conclusion

Base collector capacitances of submicron BMHBT were evaluated through microwave measurement. Smallest  $C_{BCT}$  was less than 1 fF when emitter width was 0.3  $\mu\text{m}$ . From elemental analysis of BMHBT with emitter width of 0.5  $\mu\text{m}$ , observed result could be explained when  $C_{BCin}$  is equal to  $C_{BCT}$ . Methods to improve the characteristics are also discussed.

### Acknowledgments

The authors would like to thank Professors S. Arai, M. Asada and M. Watanabe for their helpful discussions and encouragement. This work was supported by the Ministry of Education, Culture, Sports, Science and Technology through a Scientific Grant-In-Aid, the "Research for the Future" Program #JSPS-RFTF96P00101 from the Japan Society for the Promotion of Science (JSPS) and the Ministry of Public Management, Public Affairs, Posts and Telecommunications through the Grant for "Development of Frequency Resources".

### References

[1] K. Kurishima, IEEE Trans. Electron Devices, **43**, 2074 (1996).  
 [2] M. J. W. Rodwell, et al., Int. J. High-Speed Electron. Sys. **11**, 159 (2001)  
 [3] T. Arai, et al., IPRM'99, TuA1-4, Davos (1999)  
 [4] T. Arai, et al., Jpn. J. Appl. Phys. **40**, L735 (2001).  
 [5] J.M.M.Rios, et al., IEEE Trans, Microwave Theory Tech., **45**, 39, (1997).  
 [6] T. Arai, et al., IPRM'01, FA3-7, Nara (2001)

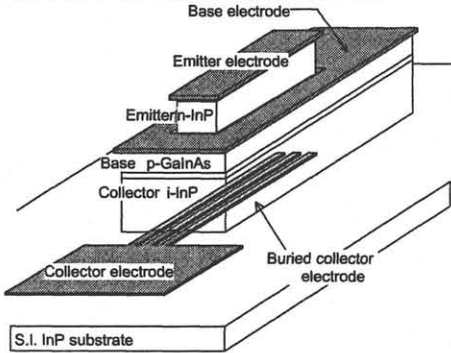


Fig.1 Schematic structure of BMHBT.

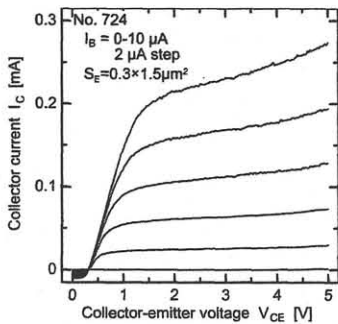


Fig.2 Common emitter characteristics of BMHBT with emitter width of 0.3  $\mu\text{m}$ .

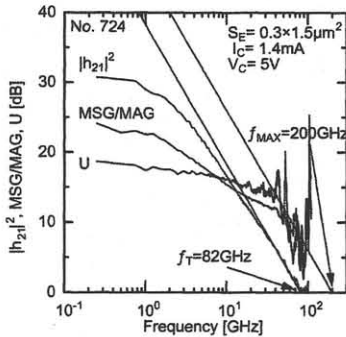


Fig.3 Microwave characteristics of BMHBT with emitter width of 0.3  $\mu\text{m}$ .

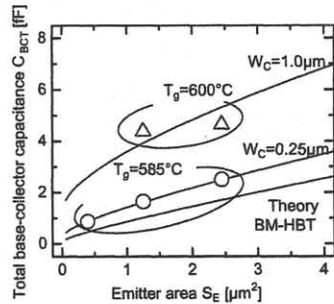


Fig.4 Estimated  $C_{BCT}$  from  $Y_{12}$  parameters. Open circles indicate present trials while open triangles indicate former trials by using higher growth temperature.

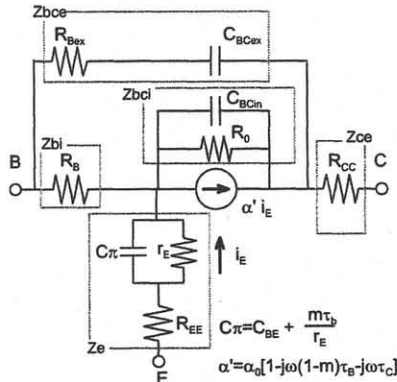


Fig.5 Using equivalent circuit.

Table 1 Estimated elements of Fig.5. Emitter area of the device is  $0.5 \times 2.5 \mu\text{m}^2$ . The bias conditions are  $I_C = 3.5 \text{ mA}$  and  $V_{CE} = 5 \text{ V}$ .

$C_{Bcin}$	1.65 [fF]	$R_0$	60000 [ $\Omega$ ]
$C_{BCext}$	0 [fF]	$R_{Bext}$	9.1 [ $\Omega$ ]
$C_{BE}$	1.47 [fF]	$\alpha_0$	0.992
$r_E$	121 [ $\Omega$ ]	$m$	0.33
$R_{EE}$	48 [ $\Omega$ ]	$\tau_B$	0.31 [ps]
$R_{CC}$	540 [ $\Omega$ ]	$\tau_C$	0.30 [ps]

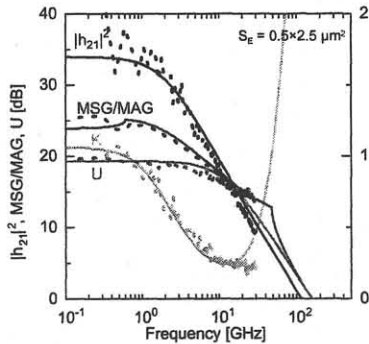


Fig.6 Simulated microwave characteristics. Measured results are shown as dots.